Optical Fiber Fabry–Perot Cavities and Recirculating Delay Lines as Tunable Microwave Filters

CHIN-LIN CHEN, SENIOR MEMBER, IEEE

Abstract—When an optical interferometer is excited by amplitude-modulated light with a sufficiently long coherence length, there may be the interference of the optical carrier and that of the modulation signals. Two interference effects can be combined to give complicated characteristics at the modulation frequency, which may be in the radio frequency or the microwave range. In this work, the radio frequency or microwave responses of single-mode fiber Fabry–Perot cavities and recirculating delay lines are studied. It is shown that fiber Fabry–Perot cavities may be used as band-pass filters and the recirculating delay lines as band-stop filters at radio or microwave frequencies. These electric filters are tunable by electro-optic effects since the band-pass or band-stop characteristic changes when the cavity or the delay line length is varied by a few tenths of an optical wavelength. The ultimate limit on speed of tuning is set by the coherence time of the light source. The dependence of the filter responses on the spectral purity of light is also studied.

I. Introduction

EVER SINCE low-loss fibers were realized two decades ago, their use has permeated into many engineering and scientific applications. For example, fibers have been used to transmit radio frequency (RF) or microwave signals and to function as electric filters, delay lines, or other signal processing devices at megahertz or gigahertz frequencies [1], [2]. Specifically, the use of optical fibers as RFdelay lines has been demonstrated by Chang *et al.* [3], and the RF and microwave characteristics of recirculating delay lines have been measured by Newton *et al.* [4], [5]. In these applications, amplitude-modulated light is fed into fibers and the output is monitored by photodetectors with sufficient speed to recover the modulation signals. In the cases cited above, either the experiments were performed with multimode fibers, or semiconductor injection lasers with relatively short coherence lengths were used as the light sources [3]–[5]. Therefore, as noted by the authors, the RF or microwave characteristics of these components depend on the interference of modulation signals imposed on the optical carrier.

If single-mode fibers are used in conjunction with highly coherent light, the interference effects of the modulation signals can be combined with the optical interference to give complicated frequency responses. Some experimental evidence has been reported by Davies *et al.* [6] and by Jackson *et al.* [7] in their work on tapped delay lines. In this work, the problems of combining optical and microwave interferences are examined in detail. Specifically, the frequency responses of Fabry–Perot cavities (FPC's) and recirculating delay lines (RDL's) are studied. We show that the frequency responses depend not only on parameters of the optical components but also on the spectral purity of the light beam. In fact, the light coherence plays an important role in determining the frequency characteristics of these components. In addition, the frequency characteristics can be tuned by varying the cavity or the loop length if the coherence length is sufficiently long. The length variation needed to tune the filter characteristics is less than a half of the optical wavelength. Such a length change, or equivalently an optical phase change, is easily achievable. If high-speed phase modulators based on electro-optic effects are inserted in the optical circuits, tuning can be very fast indeed. Ultimately, the speed of tuning is set by the coherence time of the sources.

In the following sections, the responses of fiber Fabry–Perot cavities and recirculating delay lines are analyzed. The general expressions valid for light of any spectral line shapes, together with closed-form expressions for radiation with a very narrow bandwidth, a very broad bandwidth, and a Lorentzian line shape, are obtained. Examples are given to illustrate the tunability of these electric filters. The availability of various components required to build the tunable RF or microwave filters is also reviewed.

II. RF Responses

Let the fields incident upon the fiber FPC's or RDL's be amplitude-modulated partially coherent light with a bandwidth of $\delta\omega$ centered on an angular frequency ω_0. The angular frequency of the amplitude modulation is ω_1. Thus fields impinging upon the fiber are

$$E_{in}(t) = [1 + M\cos\omega_1 t]\, e^{j\omega_0 t}\mathcal{E}(t) \tag{1}$$

where the envelop of the fields

$$\mathcal{E}(t) = \int_{-\infty}^{\infty} \tilde{\mathcal{E}}(\omega)\, e^{j\omega t}\, d\omega \tag{2}$$

Manuscript received July 11, 1989; revised October 28, 1989. This work was supported by the Indiana Corporation of Science and Technology

The author is with the School of Electrical Engineering, Purdue University, West Lafayette, IN 47907.

IEEE Log Number 8934036

varies slowly in comparison with $e^{j\omega_0 t}$. The line shape $|\tilde{\mathcal{E}}(\omega)|^2$ is left unspecified for the moment, except that it has an appreciable value only in the narrow range of $\omega_0 \pm \delta\omega/2$. A correlation function may be defined in terms of $\mathcal{E}(t)$,

$$\Gamma(\tau) = \Gamma^*(-\tau) = \langle \mathcal{E}(t)\mathcal{E}^*(t-\tau)\rangle \quad (3)$$

where brackets signify the time-averaging process. We assume that $\mathcal{E}(t)$ is normalized such that $\Gamma(0)=1$. $\Gamma(\tau)$ can be expressed in terms of the bandwidth $\delta\omega$ or the coherence length l_{coh}, which is related to $\delta\omega$ by the relation $l_{\text{coh}} \sim 2\pi c/\delta\omega$ [8].

The fields $E_{\text{tr}}(t)$ transmitted through a FPC or a RDL, just like the incident fields $E_{\text{in}}(t)$, have three spectral components, ω_0 and $\omega_0 \pm \omega_1$, and they are superimposed at the photodetector. The photodetector output is proportional to $\langle E_{\text{tr}}(t)E_{\text{tr}}^*(t)\rangle$. If the detection response time τ_d is sufficiently short, $\omega_1 \ll 1/\tau_d \ll \omega_0$, the detected signals have three frequency components: dc, ω_1, and $2\omega_1$, which are referred to as the dc, RF, and second-harmonic components respectively. The dc and second-harmonic responses are of no direct interest for the present purpose and will not be discussed further. The RF response can be expressed in terms of amplitude A_{RF} and phase ϕ_{RF} functions:

$$I_{\text{RF}}(t) = A_{\text{RF}}\cos(\omega_1 t + \phi_{\text{RF}}).$$

III. Optical Fiber Fabry–Perot Cavities

A. Analysis

Consider an optical fiber FPC with two mirrors of reflectivity r and a cavity length L. Let the effective index of refraction of the fiber be N. The dispersion of the effective index of refraction and the variation of mirror reflectivity in a narrow band $\delta\omega$ are ignored. With the input fields given by (1), the fields transmitted through the cavity are

$$E_{\text{tr}}(t) = (1-r^2)\sum_{n=0}^{\infty} r^{2n}\mathcal{E}(t_n)\left[e^{j\omega_0 t_n} + \frac{M}{2}e^{j(\omega_0+\omega_1)t_n} + \frac{M}{2}e^{j(\omega_0-\omega_1)t_n}\right] \quad (4)$$

where $t_n = t-(2n+1)T$ and $T = NL/c$ is the transit time for light to traverse the cavity. The RF component of $\langle E_{\text{tr}}(t)E_{\text{tr}}^*(t)\rangle$ is

$$I_{\text{RF}}(t) = M(1-r^2)^2\,\text{Re}\left[e^{j\omega_1 t}(T_1(t)+T_2(t))\right] \quad (5)$$

where

$$T_{1,2} = \frac{e^{-j\omega_1 T}}{1-r^4e^{-j2\omega_1 T}}\left\{\Gamma(0) + \sum_{l=1}^{\infty} r^{2l}\left[\Gamma(\pm 2lT)e^{\pm j2l\omega_0 T} + \Gamma(\mp 2lT)e^{\mp j2l(\omega_0\pm\omega_1)T}\right]\right\}. \quad (6)$$

Physically, the lth term in the series is due to the interference of waves of frequency ω_0 having completed a round-trip travel n times in the cavity with those of frequency $\omega_0 \pm \omega_1$ having journeyed the cavity $n \pm l$ times.

For light with a very broad bandwidth, $\Gamma(\tau)=0$ for $\tau \neq 0$. The amplitude function of the RF component can be deduced immediately from (5) and (6):

$$A_{\text{RF}} = 2M(1-r^2)^2\left[1+r^8-2r^4\cos 2\omega_1 T\right]^{-1/2}. \quad (7)$$

It is due to the interference of the modulation signals only. This is expected since the optical interference is not observable in the limit of $\delta\omega \to \infty$. The peaks of A_{RF} occur at $f_{p1} = mc/(2NL)$, where m is an integer. The full width between points of half maximum is, for $r > 3^{-1/4}$,

$$\Delta f_{1p} = \frac{c}{\pi NL}\sin^{-1}\frac{\sqrt{3}(1-r^4)}{2r^2}$$

and it is independent of optical frequency ω_0.

B. Discussion

For signals with a Lorentzian line shape, $\Gamma(\tau) = e^{-|\delta\omega\tau|}$, the series in (6) can be summed in closed form and we have

$$A_{\text{RF}} = \frac{M(1-r^2)^2}{\left(1+r^8-2r^4\cos 2\omega_1 T\right)^{1/2}} \cdot \left|\left[2 + \frac{r^2e^{-2(\delta\omega-j\omega_0)T}}{1-r^2e^{-2(\delta\omega-j\omega_0)T}} + \frac{r^2e^{-2(\delta\omega+j\omega_0)T}}{1-r^2e^{-2(\delta\omega+j\omega_0)T}} + \frac{r^2e^{-2(\delta\omega+j(\omega_0+\omega_1))T}}{1-r^2e^{-2(\delta\omega+j(\omega_0+\omega_1))T}} + \frac{r^2e^{-2(\delta\omega-j(\omega_0-\omega_1))T}}{1-r^2e^{-2(\delta\omega-j(\omega_0-\omega_1))T}}\right]\right|. \quad (8)$$

Equation (8) reduces to (7) in the limit of $\delta\omega \to \infty$. The case of very narrow bandwidth can also be obtained from (8) by letting $\delta\omega \to 0$. Equations (7) and (8) can also be expressed in terms of NL/λ_0, NL/λ_1, and NL/l_{coh}, since $\omega_0 T = 2\pi NL/\lambda_0$, $\omega_1 T = 2\pi NL/\lambda_1$, and $\delta\omega T = 2\pi NL/l_{\text{coh}}$, where λ_0 and λ_1 are free-space wavelengths at angular frequencies ω_0 and ω_1 respectively. To study the dependence of A_{RF} on the cavity length, the mirror reflectivity, and the light coherency, A_{RF} is plotted as a function of ω_1 with r, $\omega_0 T$, and $\delta\omega T$ as parameters. Typical results are shown in Figs. 1 and 2. Examination of (8) reveals that A_{RF} is large when the cavity length is exactly an integer multiple of $\lambda_0/(2N)$. Therefore we begin by studying the responses of a cavity with $NL/\lambda_0 = m$ and they are shown as the solid lines in Figs. 1 and 2. More specifically, we choose $m = 157977$, which corresponds to a cavity with $NL \sim 10$ cm and is excited by light with $\lambda_0 = 0.633$ μm. As noted previously, the fields contain three spectral components: ω_0 and $\omega_0 \pm \omega_1$. The peaks of the solid lines correspond to cavities which resonate at ω_0 and $\omega_0 \pm \omega_1$ simultaneously. To facilitate comparison, all curves, including the broken lines to be discussed shortly, are normalized with respect to peaks of the solid curves. Generally speaking, when the coherence length is comparable to or shorter than NL, the responses are determined mainly by the interference of modulation signals, and are insensitive to minute changes in the cavity

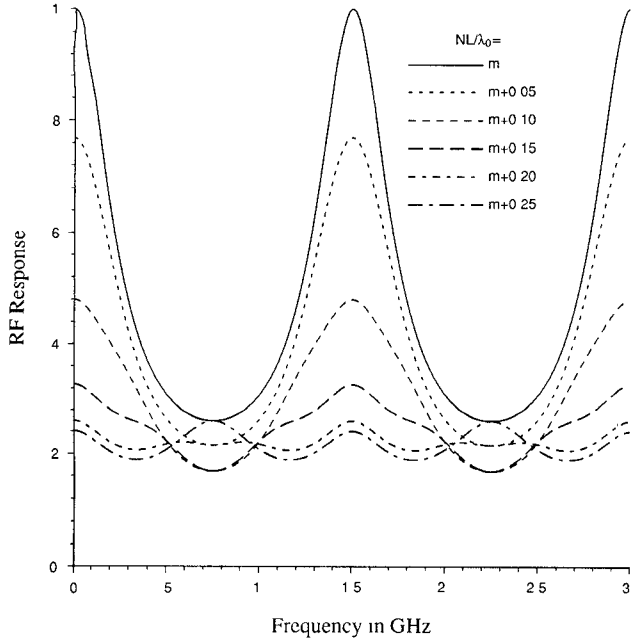

Fig. 1. RF responses of FPC's with $r = 0.8$, $NL \sim 10.0$ cm excited by light with $l_{coh} = 20NL$.

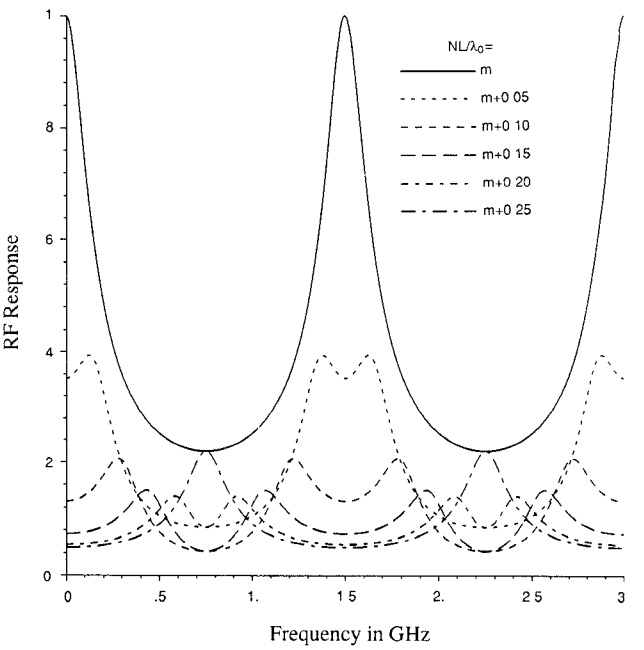

Fig. 2 RF responses of FPC's with $r = 0.8$, $NL \sim 10.0$ cm excited by light with $l_{coh} = 2000NL$.

length. If l_{coh} is longer than $20NL$, the difference in response becomes apparent as the cavity length varies. The dotted and dashed lines in Figs. 1 and 2 correspond to cavities with $NL/\lambda_0 = m + 0.05$, $m + 0.10$, $m + 0.15$, $m + 0.20$, and $m + 0.25$. Note that the length changes are only fractions of λ_0/N. As l_{coh} increases, the effects of the optical interference become more evident. In all cases studied, the responses with $l_{coh} \geq 200NL$ are very similar to those with $l_{coh} = 2000NL$ (Fig. 2) except for the fine details. The responses with $l_{coh} \geq 2000NL$ are identical to cases where the coherence length is infinitely long.

IV. Recirculating Delay Lines

A. Analysis

The heart of a fiber RDL is a 2×2 fiber directional coupler. The inputs and outputs of a lossless coupler are related by a unitary matrix. In its most general form, a 2×2 unitary matrix is given by, as noted by Hurwitz and Jones [9],

$$\begin{bmatrix} A & B \\ -B^* & A^* \end{bmatrix}$$

where A and B are complex variables and $|A|^2 + |B|^2 = 1$. To account for possible power loss in the coupler, we use $|A|^2 + |B|^2 = 1 - \gamma$, with γ representing the percentage of power loss in the coupler. Thus for lossy couplers made of identical, nonbirefringent fibers and in the absence of twisting in the coupling region [10]–[15], A and B are

$$A = \sqrt{(1-\gamma)(1-\kappa^2)} \tag{9a}$$

$$B = j\kappa\sqrt{1-\gamma}\,. \tag{9b}$$

Let L be the length of the fiber delay line. The coupler length is ignored since it is relatively short in comparison with L. With the input to the RDL given by (1), the output is

$$E_{tr}(t) = \frac{|A|^2}{B}\sum_{n=0}^{\infty} C_n \mathscr{E}(t_n') \cdot \left[e^{j\omega_0 t_n'} + \frac{M}{2}e^{j(\omega_0+\omega_1)t_n'} + \frac{M}{2}e^{j(\omega_0-\omega_1)t_n'}\right] \tag{10}$$

where $C_0 = -|B/A|^2$, $C_n = B^n$ for $n \geq 1$, $t_n' = t - nT$, and $T = NL/c$.

Following the same method used previously in analyzing the FPC, we obtain an expression for the RF component of the detector output:

$$I_{RF}(t) = M\frac{|A|^4}{|B|^2}\mathrm{Re}\left[e^{j\omega_1 t}(T_3 + T_4)\right] \tag{11}$$

where

$$T_3 = \Gamma(0)\left[\left|\frac{B}{A}\right|^4 + \frac{|B|^2 e^{-j\omega_1 T}}{1-|B|^2 e^{-j\omega_1 T}}\right] + \left[-\left|\frac{B}{A}\right|^2 + \frac{|B|^2 e^{-j\omega_1 T}}{1-|B|^2 e^{-j\omega_1 T}}\right] \cdot \sum_{l=1}^{\infty}\left[(B^*)^l \Gamma(lT)\, e^{jl\omega_0 T} + B^l \Gamma(-lT)\, e^{-jl(\omega_0+\omega_1)T}\right] \tag{12}$$

$$T_4 = \Gamma(0)\left[\left|\frac{B}{A}\right|^4 + \frac{|B|^2 e^{-j\omega_1 T}}{1-|B|^2 e^{-j\omega_1 T}}\right] + \left[-\left|\frac{B}{A}\right|^2 + \frac{|B|^2 e^{-j\omega_1 T}}{1-|B|^2 e^{-j\omega_1 T}}\right] \cdot \sum_{l=1}^{\infty}\left[(B^*)^l \Gamma(lT)\, e^{jl(\omega_0-\omega_1)T} + B^l \Gamma(-lT)\, e^{-jl\omega_0 T}\right]. \tag{13}$$

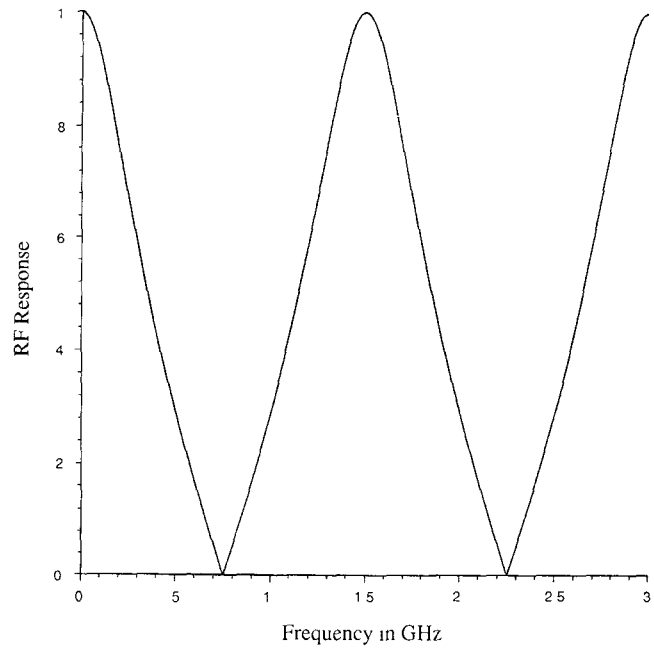

Fig. 3. RF responses of RDL's with $\kappa = 0.5723$, $\gamma = 0.05$, $NL \sim 20.0$ cm excited by light with $l_{coh} = NL$.

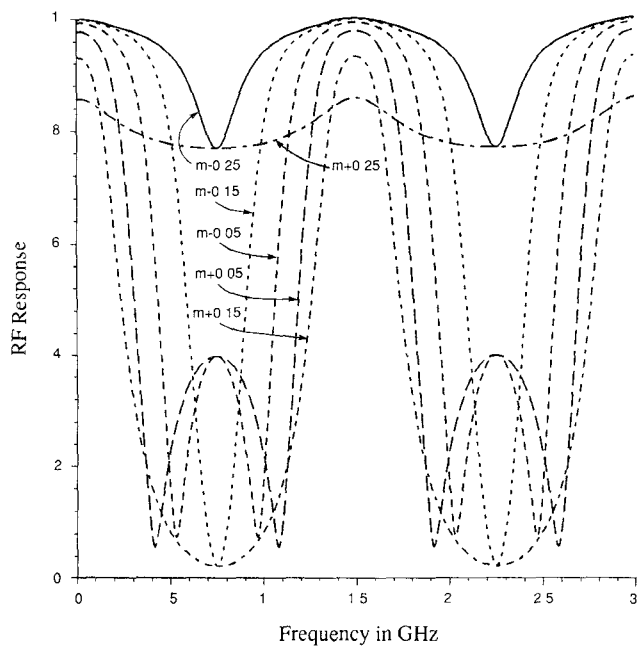

Fig 4. RF responses of RDL's with $\kappa = 0.5723$, $\gamma = 0.05$, $NL \sim 20.0$ cm excited by light with $l_{coh} = 100NL$.

If the coherence length is very short, the amplitude function of the RF response can be written as

$$A_{RF} = 2M\left\{\frac{\left(|A|^4 - |B|^4 + |B|^2\right)^2 - 4|B|^2\left(|A|^4 - |B|^4\right)\sin^2\frac{\omega_1 T}{2}}{\left(1-|B|^2\right)^2 + 4|B|^2\sin^2\frac{\omega_1 T}{2}}\right\}^{1/2}. \quad (14)$$

The fact that A_{RF} is independent of $\omega_0 T$ is a clear indication that it is the result of interference of modulation signals only. A_{RF} has notches at $NL = (m + 1/2)\lambda_1$ with a minimum value of

$$A_{RF\,min} = 2M\left|\frac{|A|^4 - |B|^4 - |B|^2}{1+|B|^2}\right|.$$

If $|A|^4 = |B|^4 + |B|^2$, $A_{RF\,min}$ vanishes; i.e., the notches become nulls. If we choose A and B given in (9a) and (9b), the condition for vanishing $A_{RF\,min}$ reduces to $\kappa^2 = (1-\gamma)/(3-2\gamma)$. In other words, sharp notches occur if the loss in the RDL is small and $\kappa^2 \sim 1/3$.

B. Discussion

For light with a Lorentzian spectral line shape, the amplitude function can be simplified:

$$A_{RF} = M|A|^4\left|2\left(\frac{|B|^2}{|A|^4} + \frac{e^{-j\omega_1 T}}{1-|B|^2 e^{-j\omega_1 T}}\right) + \left(-\frac{1}{|A|^2} + \frac{e^{-j\omega_1 T}}{1-|B|^2 e^{-j\omega_1 T}}\right) \cdot \left\{\frac{B^* e^{-(\delta\omega - j\omega_0)T}}{1-B^* e^{-(\delta\omega - j\omega_0)T}} + \frac{B e^{-(\delta\omega + j\omega_0)T}}{1-B e^{-(\delta\omega + j\omega_0)T}} + \frac{B e^{-(\delta\omega + j(\omega_0+\omega_1))T}}{1-B e^{-(\delta\omega + j(\omega_0+\omega_1))T}} + \frac{B^* e^{-(\delta\omega - j(\omega_0-\omega_1))T}}{1-B^* e^{-(\delta\omega - j(\omega_0-\omega_1))T}}\right\}\right|. \quad (15)$$

The first term of (15) is due to the interference of modulation signals alone. The effects of the optical interference are represented by the second term by the presence of $\omega_0 T$ and $\delta\omega T$ terms. Again, the case of infinitesimal bandwidth can be deduced from (15) by reducing $\delta\omega$ to 0.

Figs 3 and 4 depict the RF responses of RDL's with $NL \sim 20$ cm, $\kappa = 0.5723$, and $\gamma = 0.05$ for $l_{coh} = NL$ and $100NL$. A loop length of approximately $20/N$ cm is chosen so that the round-trip optical length of the RDL's is the same as that of the FPC's studied in the last section. The RF responses are the strongest when the loop length is $(m - 0.25)\lambda_0/N$, where m is an integer, and these responses are also plotted as solid curves. All curves are normalized with respect to the peaks of the solid lines. As indicated in (9b), there is a phase delay of $\pi/2$ in coupling light from one fiber of the coupler to another fiber. Thus constructive interference occurs if the delay line is a fourth of λ_0/N shorter than an integer multiple of λ_0/N. The response becomes weaker as the loop length deviates from $(m - 0.25)\lambda_0/N$, and it is the weakest when $L = (m + 0.25)\lambda_0/N$. The notches shown in Fig. 3 are very deep because of the values of κ and γ chosen. The effect of optical interference is not noticeable if $l_{coh} \sim NL$. As l_{coh} increases, the effect of optical interference becomes increasingly apparent. In particular the minima are quite sensitive to the changes in NL when l_{coh} is longer than $10NL$. But the peaks do not change very much when NL or l_{coh} varies.

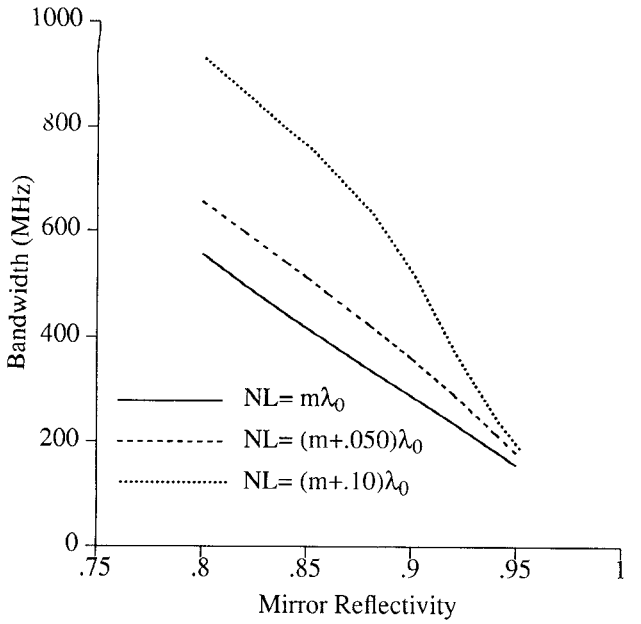

Fig. 5. Bandwidth of band-pass filters based on FPC's with $NL \sim 10.0$ cm and $l_{coh} = 20NL$.

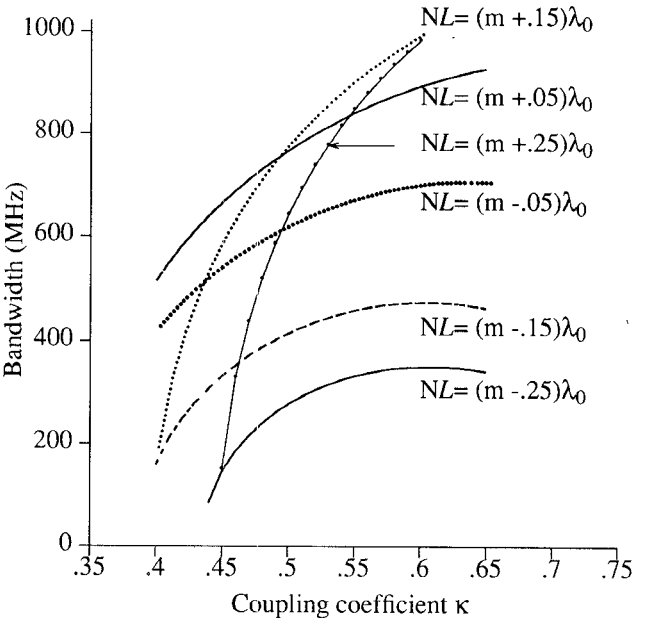

Fig. 6. Bandwidth of band-stop filters based on RDL's with $\gamma = 0.05$, $NL \sim 20.0$ cm, and $l_{coh} = 10NL$.

V. Tunable RF Filters and Remarks

As shown in (8) and (15), A_{RF} of FPC's is the product of two terms and that of RDL's is the sum of two terms. In both cases, one term is due to the interference of the modulation signals while the other contains the effect of the optical interference. The mirror reflectivity, or κ and γ of the couplers, affects both the optical interferences and that of the modulation signals. But the coherence length affects only the optical interference term.

Although the results shown in Figs. 1–4 are for specific values of m, they are valid representations of the responses for all values of m so long as m is large. Examination of these figures reveals that FPC's may be used as band-pass filters and RDL's as band-stop filters.

A. Two Examples

For example, the RF response of the FPC shown as the solid line in Fig. 1 has the characteristic of a band-pass filter with center frequencies at 1.5 GHz and all integer multiples of 1.5 GHz, and a passband (full width between half maximum points) of 556 MHz. If the cavity length is increased by 0.05 or 0.10 λ_0/N (the dotted and dashed curves in Fig. 1), the passband increases to 656 or 928 MHz respectively.

In general, the center frequency is determined by the cavity length and the effective index of refraction. The width of the passband decreases as the mirror reflectivity increases, as shown in Fig. 5. As the coherence length increases, the characteristics in the passband may become quite complicated.

To illustrate the use of RDL's as notch filters, consider the responses of RDL's shown as dotted and dot–dash curves in Fig. 4. As the loop length varies from $(m - 0.15)\lambda_0/N$ to $(m + 0.15)\lambda_0/N$, the width of the stopband increases from 470 MHz to 944 MHz. The center frequency remains unchanged. Calculations show that the bandwidth depends strongly on the coupling coefficient κ (Fig. 6) and is rather insensitive to the variation in coupler loss γ. The maximum rejection, i.e., the minimum of the response, is determined by κ, γ, and $l_{coh}/(NL)$.

B. Remarks

The building blocks of tunable filters are optical sources with a long coherence length, means to modulate the optical signals, fibers with built-in or attached mirrors to form Fabry–Perot cavities or fiber directional couplers to form recirculating delay lines, mechanisms to alter the cavity or the loop lengths or the optical phase in the fiber circuit, and high-speed photodetectors. As with any optical interferometric device, the performance of these filters may be vulnerable to environmental disturbance. To realize their full potential, it may be necessary to utilize some stabilizing or feedback scheme to minimize the environmental effects [7]. For all light sources, including semiconductor injection lasers, wide-band modulators based on $LiNbO_3$ or other electro-optic materials may be used as external modulators to effect modulation [16]. Dielectric or metallic mirrors have been deposited directly onto fiber ends [17], [18]. Fiber Fabry–Perot cavities with a finesse of 500 have been formed by attaching dielectric mirrors to the fibers [19]. Single-mode fiber couplers with various degrees of coupling and loss are available commercially and fiber RDL resonators with a finesse of 1260 have been reported recently [20]. In addition, p-i-n photodiodes with bandwidths in excess of 20 GHz are also available to detect radiation of 0.6–0.85 μm [21] or 1.0–1.6 μm [22]. In

the examples cited previously, the change in cavity or loop length required to tune the filters is less than $0.3\ \lambda_0/N$, or an optical phase change less than 2 rad. The length change may be accomplished by stretching or compressing the fibers piezoelectrically, or electro-optic phase shifters may be inserted into the optical path to vary the optical phase delay electrically. Thus the only building block left is light sources with a long coherence length. For applications in the 1 to 10 GHz range, NL of RDL or $2NL$ of FPC is between 1.5 and 15 cm. As noted previously, the interference of optical signals and that of modulation signals may be combined if the coherence length is 10 times $2NL$ of the FPC or NL of the RDL or longer. Thus the coherence length required is on the order of a few meters. A coherence length of 5 m corresponds to a spectral line width of 60 MHz. The spectra of gas lasers are quite narrow, particularly those having etalons in the laser cavities, and no further comment is necessary. For conventional single-mode single-frequency DH lasers at 0.85 μm, the spectral width is in the 80 to 100 MHz range [23]. Several schemes have been conceived to improve the spectral purity; these include the use of single quantum well structures as the lasing medium [24], gratings to provide the distributed feedback or to function as distributed Bragg reflectors [25], and external cavities used as part of the laser cavity [23]. For state-of-the-art DFB lasers emitting at 1.55 μm, the line width may be as narrow as 1.7 MHz [26]. In the presence of an external cavity, the line width of a conventional single-mode DH laser can be reduced to 15 to 20 kHz [23]. It has also been reported that by incorporating a long passive cavity on the same semiconductor wafer, a line width of 0.6 MHz with a center wavelength of 1.27 μm has been obtained [27]. Although direct and broad-band modulation is possible for semiconductor injection lasers [28], the conditions for broad-band modulation may conflict with those for narrow spectral width. In those cases, broad-band external modulators may be used. In short, semiconductor laser technology has matured sufficiently that the requirement for narrow spectral lines can be met easily.

In summary, we note that effects of optical and modulation interferences in FPC's or RDL's can be combined if light is sufficiently coherent. When two interference effects are combined, the fiber components may have band-pass or band-stop characteristics in the radio frequency or microwave ranges. In particular, FPC's may be used as band-pass filters and RDL's as band-stop filters. Furthermore, the filtering characteristics may be tuned by varying the length of the optical circuit. A change in fractions of the optical wavelength is sufficient for this purpose. The needed length variation is obtainable by using piezoelectric materials such as PZT ceramics or copolymers of vinylideene fluoride (PV_2) films to stretch or compress the fibers. For fiber components tuned piezoelectrically, the speed of tuning is limited by the speed of the piezoelectric materials, which is in the millisecond range. If high-speed operations are desired, electro-optic phase shifters may be inserted into the optical circuit to vary the optical phase. The ultimate limit of these filters is the coherence time.

REFERENCES

[1] B. Moslehi, J. W. Goodman, M Tur, and H. J Shaw, "Fiber-optic lattice signal processing," *Proc. IEEE*, vol 72, no. 7, pp. 909–930, 1984.

[2] K. P. Jackson *et al*, "Optical fiber delay-line signal processing," *IEEE Trans Microwave Theory Tech.*, vol MTT-33, pp. 193–209, Mar 1985.

[3] C T. Chang, J A Cassaboom, and H. F Taylor, "Fibre-optic delay line devices for R. F. signal processing," *Electron. Lett.*, vol. 13, no. 22, pp 678–680, 1977.

[4] J. E Bowers, S. A. Newton, W. V Sorin, and H. J. Shaw, "Filter response of single-mode fibre recirculating delay lines," *Electron Lett.*, vol. 18, no. 3, pp. 110–111, 1982.

[5] S. A. Newton and P. S Cross, "Microwave-frequency response of an optical-fibre delay line filter," *Electron Lett.*, vol 19, no. 13, pp. 480–481, 1983.

[6] D. E N Davies and G. W. James, "Fibre-optic tapped delay line filter employing coherent optical processing," *Electron. Lett*, vol. 20, no. 2, pp. 95–97, 1984.

[7] K. P. Jackson, G. Xiao, and H. J. Shaw, "Coherent optical fibre delay line processor," *Electron. Lett.*, vol. 22, no 25, pp. 1335–1337, 1986.

[8] M. Born and E. Wolf, *Principles of Optics*, 6th ed New York: Pergamon Press, 1980, ch 10.

[9] H. Hurwitz and R. C. Jones, "A new calculus for the treatment of optical systems, II: Proof of three general equivalence theorems," *J Opt Soc Amer.*, vol 31, pp. 493–499, 1941.

[10] C. L Chen and W. K Burns, "Polarization characteristics of single-mode fiber couplers," *IEEE J. of Quantum Electron.*, vol QE-18, pp. 1589–1600, 1982.

[11] L F Stokes, M. Chodorow, and H. J. Shaw, "All-single-mode fiber resonator," *Opt. Lett.*, vol. 7, no. 6, pp. 288–290, 1982.

[12] B. Crosignani, A Yariv, and P. Di Porto, "Time-dependent analysis of fiber-optic passive loop resonators," *Opt Lett*, vol. 11, no. 6, pp. 251–253, 1986.

[13] Z. K Ioannidis, P. M. Radmore, and I. P. Giles, "Dynamic response of an all-fiber ring resonator," *Opt Lett.*, vol. 13, no 5, pp. 422–424, 1986.

[14] Y. Ohtsuka, "Analysis of a fiber-optic passive loop resonator gyroscope: Dependence on resonator parameters and light-source coherence," *J. Lightwave Technol*, vol LT-3, pp 378–384, 1985.

[15] Y Ohtsuka, "Optical coherence effects on a fiber-sensing Fabry-Perot interferometer," *Appl. Opt.*, vol 21, pp 4316–4320, 1982.

[16] H Haga, "$LiNbO_3$ traveling wave light modulator/switch with etched groove at the electrode gap," *IEEE J of Quantum Electron.*, vol QE-22, pp. 902–906, 1986

[17] C E Lee and H F. Taylor, "Interferometric sensors using internal mirrors," *Electron Lett.*, vol. 24, pp 193–194, 1988.

[18] S. M. Tseng and C L. Chen, "Optical fiber Fabry-Perot sensors," *Appl Opt*, vol 27, pp 547–551, 1988

[19] J Stone and D. Marcuse, "Ultrahigh finesse fiber Fabry–Perot interferometers," *J Lightwave Technol.*, vol LT-4, pp. 382–385, 1986

[20] C. Y. Yue, J. D. Peng, Y. B. Liao, and B. K Zhou, "Fiber ring resonator with finesse of 1260," *Electron Lett.*, vol 24, pp. 622–623, 1989.

[21] S. Y Wang, D M. Bloom, and D. M. Collin, "20-GHz bandwidth GaAs photodiode," *Appl. Phys. Lett.*, vol. 42, pp 190–192, 1983

[22] J. E. Bowers, C. A. Burrs, and R. J McCoy, "InGaAs PIN photodetectors with modulation response to millimetre wavelengths," *Electron. Lett*, vol. 21, pp. 812–814, 1985.

[23] A. Mooradian, "Laser linewidth," *Physics Today*, pp 42–48, 1985

[24] Y. Arakawa and A Yariv, "Theory of gain, modulation response, and spectral linewidth in AlGaAs quantum well lasers," *IEEE J. Quantum Electron*, vol. QE-21, pp. 1666–1674, 1985

[25] I. Mito, "Recent advances in frequency tunable DFB–DBR lasers," in *Proc 1988 Opt. Fiber Commun* (New Orleans, LA), 25–28 Jan 1988, paper THK1

[26] K. Sato, Y Kondo, M. Nakao, and M. Fukuda, "1.55 μm narrow-linewidth and high-power DFB lasers for coherent transmission

systems," in *Proc. 1989 Opt. Fiber Commun.* (Houston, TX), 6–9 Feb. 1989, paper TUH6.

[27] Y. Matsui *et al.*, "Narrow spectral linewidth integrated-passive-cavity laser," in *Proc. 1988 Opt. Fiber Commun.* (New Orleans, LA), 25–28 Jan. 1988, paper THK7.

[28] K. Y. Lau. and A. Yariv, "Ultra-high speed semiconductor lasers," *IEEE J. Quantum Electron.*, vol. QE-21, pp. 121–138, 1985.

✠

Chin-Lin Chen (S'64–M'66–SM'87) received the B.S.E.E. degree from National Taiwan University, Taipei, China, in 1958, the M.S. degree from North Dakota State University, Fargo, in 1961, and the Ph.D. degree from Harvard University, Cambridge, MA, in 1965.

From 1965 to 1966, he was a Research Fellow in the Division of Engineering and Applied Physics, Harvard University. In 1966, he joined the School of Electrical Engineering, Purdue University, West Lafayette, IN, as an Assistant Professor. He is currently a Professor of Electrical Engineering there. He has been on sabbatical leave at the University of California at Berkeley and at the Naval Research Laboratory, Washington, DC. His research interests are in the areas of scattering and diffraction of electromagnetic waves, antenna radiation, surface acoustic wave filters and cavities, integrated and fiber-optical components, and optical fiber sensors.

Dr. Chen is a member of Sigma Xi, Eta Kappa Nu, the American Society for Engineering Education, and the U.S. National Committee for the International Union of Radio Science.